Met. Mater. Int., Vol. 20, No. 2 (2014), pp. 243~248
doi: 10.1007/s12540-014-2006-9

High Temperature High Cycle Fatigue Behavior of New Aluminum Alloy Strengthened by $(Co, Ni)_3Al_4$ Particles

Kyu-Sik Kim[1], Si-Young Sung[2], Bum-Suck Han[2], Chang-Yeol Jung[3], and Kee-Ahn Lee[1,*]

[1]Andong National University, School of Advanced Materials Engineering, Andong 760-749, Korea
[2]Korea Automotive Technology Institute, Cheonan 330-912, Korea
[3]Dongguk University, Gyeongju 780-714, Korea

(received date: 29 July 2013 / accepted date: 16 September 2013)

High cycle fatigue (HCF) behavior of a new heat-resistant aluminum alloy at elevated temperature was investigated. This alloy consists of an α-Al matrix, a small amount of precipitated Mg_2Si, and distributed $(Co, Ni)_3Al_4$ strengthening particles. HCF tests were conducted with a stress ratio of (R)=0 and a frequency of (F)=30 Hz at 130 ℃. The fatigue limit (maximum stress) of this alloy was 120 MPa at 10^7 cycles. This is a value superior to that of conventional heat-resistant aluminum alloys such as the A319 alloy. Furthermore, regardless of the stress conditions, the new heat-resistant Al alloy has an outstanding fatigue life at high temperatures. The results of fractography observation showed that second phases, especially $(Co, Ni)_3Al_4$ particles, were effective to the resistance of fatigue crack initiation and propagation. On the other hand, Mg_2Si particles were more easily fractured by the fatigue crack. This study also clarifies the micromechanism of fatigue deformation behavior at elevated temperature related to its microstructure.

Key words: alloys, casting, fatigue, scanning electron microscopy

1. INTRODUCTION

Recently, aluminum alloys have been re-focused as a lightweight material for automobiles and aviation because of its superiority in strength to weight, mechanical properties, formability and recyclable merit. Heat-resistant Al alloys have been used for engine heads, cylinder heads, and cylinder blocks [1]. Much development and many studies are still ongoing for the purpose of improving heat-resistant stability and high temperature mechanical and fatigue properties.

Currently, the most commonly used heat-resistant Al alloy includes Al-Si-based A319, A356, and A309 alloys [2]. These alloys have superior castability and demonstrate good high temperature mechanical properties through the existence of eutectic Si particles, precipitation hardening and solid solution hardening achieved by addition of small amounts of alloying elements. However, as the temperature and exposure time increase, microstructural changes, e.g., decomposition and growth of precipitates and eutectic Si particles, occur; thus, the high temperature mechanical properties deteriorate [3,4]. Therefore, there is a need to develop Al alloys that have superior properties under high temperatures and cyclic stress.

Studies have been conducted on changing the composition of Al alloys and modifying hardening mechanisms to enhance the high temperature mechanical and fatigue properties [5-9]. First, in relation to changes in alloy composition and grain size, Moffat *et al.* [5] reported that the high-temperature fatigue crack propagation of Al-Si alloys had partial resistance with an increasing Si content but faster crack propagation in high-stress conditions. Canadinc *et al.* [6] studied the high-temperature cyclic deformation property of Al-Mg alloys - which have very small grain size - and reported that grain growth occurred as temperature increased; that resulted in deteriorating high-temperature fatigue properties. Recently, some studies have reported that heavily alloyed Al alloys that have many additional alloying elements, such as Cu, Ti, Mn, Zr, V, and Ce, have superior mechanical properties at high temperature, and these have been drawing renewed attention [7-9]. According to the results published by Zhang *et al.* [7] and A.M.A. Mohamed *et al.* [8], as diverse alloy elements are added, various kinds of intermetallic compounds are formed in the microstructures of the aluminum alloys. Although intermetallic compounds sometimes act as reinforcement phases that improve the tensile strength of aluminum alloys at high temperatures, they generally have brittle characteristics and adverse effects on fatigue properties. Other researchers studied high temperature fatigue properties of dispersion hardened Al alloys. In studying such properties of dispersion hardened composite materials, Uematsu *et al.* [10]

*Corresponding author: keeahn@andong.ac.kr

and Sugimura and Suresh [11] investigated the effect of size and volume fraction of SiC particles on the high temperature fatigue properties of dispersion hardened Al-Cu-based alloys. Their results demonstrated partial enhancement of the high-temperature fatigue properties in low-stress conditions but deteriorating fatigue properties in the high-stress regime. Hartmann *et al.* [12] used the 6061-T6 alloy hardened by distributed Al_2O_3 particles, which also showed characteristics similar to composite materials with dispersion-hardened SiC particles. Several other studies have been conducted on the high temperature fatigue properties of aluminum-based composite alloys [13-15]. Their results, however, revealed that aluminum-based composite materials are not effective in terms of high temperature fatigue properties despite their superiority to typically used aluminum alloys in terms of a high temperature tensile property and wear resistance. There is a need to develop new heat-resistant Al alloys that demonstrate superior high temperature fatigue properties, and research must be conducted on the fatigue fracture mechanism in connection with the microstructure to enhance the high temperature fatigue properties.

This study presents a new Al-1%Mg-1.1%Si (wt%)-based aluminum alloy that is heat-resistant, aluminum alloy-distributed, and has Co-Ni base particles. We investigated the microstructure and high cycle fatigue properties of the new heat-resistant aluminum alloy in this study. We also discuss the deformation and fracture mechanism of the new heat-resistant aluminum alloy as they relate to its microstructure.

2. EXPERIMENTAL PROCEDURES

This study used an Al alloy composed of Al-1%Mg-1.1%Si-0.8%CoNi (wt%) [16]. The Al-Mg-Si-0.8%CoNi alloy was manufactured using powder ball milling, high frequency induction melting and continuous casting. First, pure Co and pure Ni powders (manufactured by a powder metallurgy process of atomization) were mixed and prepared by the ball milling process for one hour. These powders were added to the pure Al melts to manufacture the Al-3%CoNi master alloy. This master alloy was re-melted, and Al, Mg, and Si were added to adjust the Al-1%Mg-1.1%Si-0.8%CoNi (wt%) composition. It was directly manufactured into billets by continuous casting. Then, additional heat treatments (510 °C/2 h and then 190 °C/8 h) were conducted. A 1 ml HF + 99ml H_2O solution was used for etching; optical microscopy and scanning electron microscopy (JEOL JSM-6300) were used to observe the microstructure. In addition, X-Ray Diffraction (XRD) analysis, Energy Dispersive Spectroscopy (EDS), and High Resolution-Transmission Electron Microscopy (HR-TEM) were used to perform a phase analysis. Differential Thermal Analysis (DTA) was conducted to check the thermal stability of the alloy with an increasing temperature from room temperature to 900 °C (heating rate =10 K/min).

All specimens were prepared according to ASTM E466, and Fig. 1 shows the size and shape of the specimens for the high-cycle fatigue used in this study. Before testing, the gauge was polished using #2000 SiC paper to minimize the effect of surface roughness (surface roughness: below ~2 μm). The high-temperature, high cycle fatigue test was conducted using MTS 810 servo-hydraulic equipment at 130 °C through uniaxial stress control with a stress ratio of R=0 (tension-zero condition) and frequency = 30 Hz. The high cycle fatigue limit was set from 10^7 cycles to the maximum stress at which fractures did not occur, with the average fatigue life set after three tests at the same maximum stress. After the fatigue test, scanning electron microscopy (SEM) was used to check the fatigue fracture surfaces. The vertical cross-section of the fractured surface was also observed to examine the high-temperature fatigue crack propagation behavior.

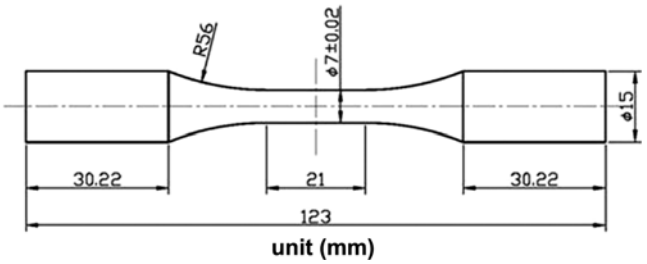

Fig. 1. Specimen size and shape for high cycle fatigue test at elevated temperature.

3. RESULTS AND DISCUSSION

3.1. Microstructure and phase analysis of new heat resistant Al alloy

Figure 2 presents the microstructure of the new Al alloy. As shown in Fig. 2(a), grains of the alloy had a size range of 40-400 μm and an average value of 185 μm. Figure 2(b) shows the bright particles observed together with the dark particles, which existed in the α-Al matrix. The bright particles were elongated in directions similar to a matrix, and they had an average size of 1.57 μm. Moreover, the bright particles were evenly distributed inside the alloy with an average inter-particle distance of 17.4 μm. In contrast, the dark particles showed a

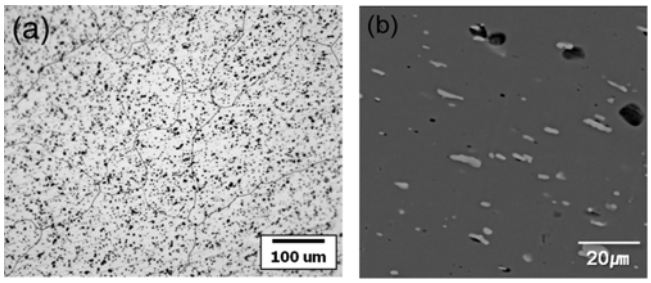

Fig. 2. Microstructure of new heat resistant Al alloy; (a) observed by optical microscope after etching and (b) by SEM before etching [16].

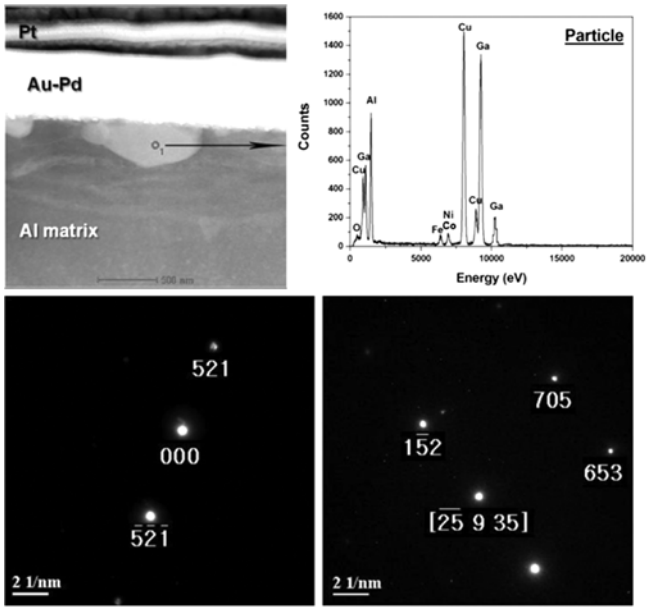

Fig. 3. Phase analysis results of dispersed particle (white) in new Al alloy by using HR-TEM [16].

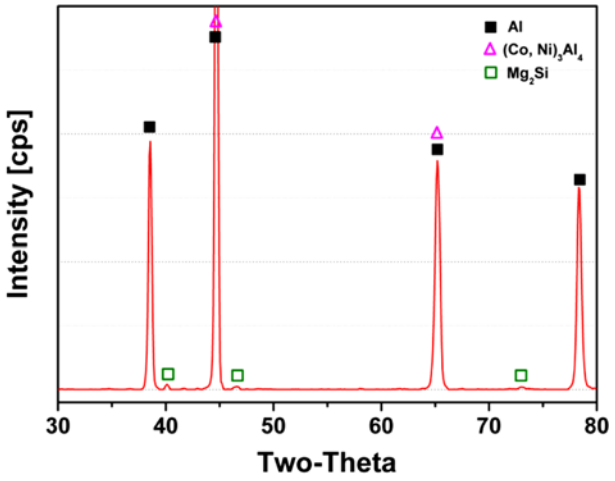

Fig. 4. Result of the X-ray diffraction analysis of new Al alloy.

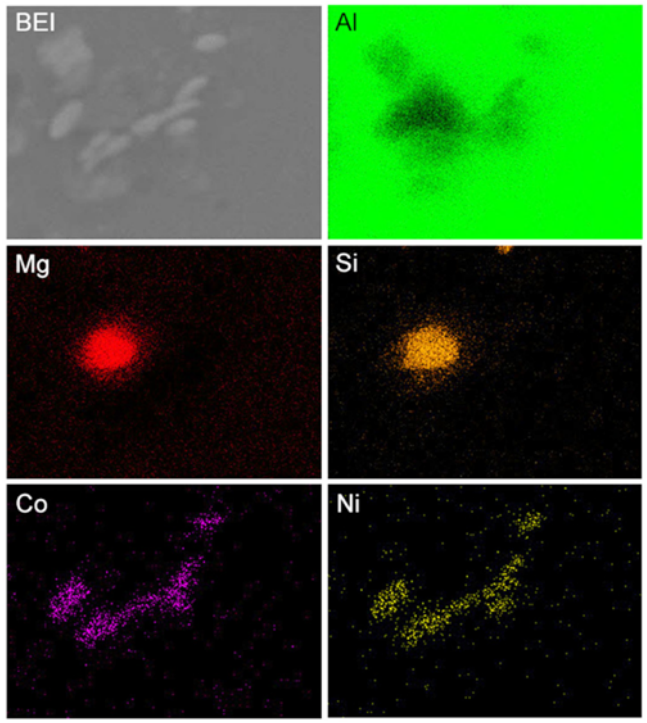

Fig. 5. EDS mapping results of the particle existed in new Al alloy.

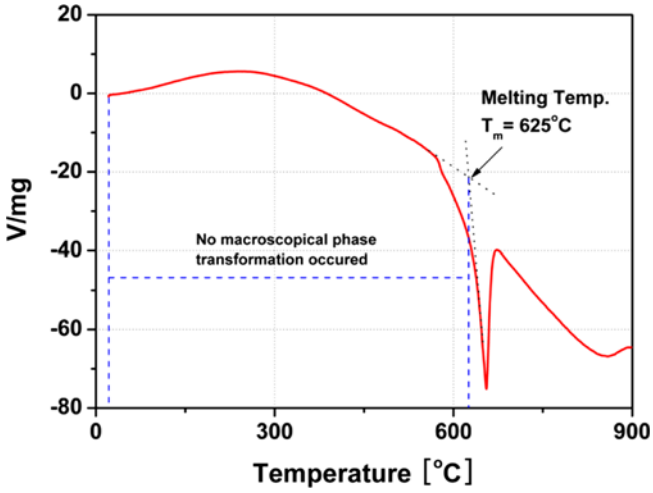

Fig. 6. DTA analysis result of new Al alloy from R.T. to 900 °C.

relatively spherical morphology and had a bigger average size (~10 μm) than the bright phase. The bright particle sampled using a Focus Ion Beam (FIB) were analyzed through High Resolution-Transmitted Electron Microscopy (HR-TEM) for the phase analysis, and the results are shown in Fig. 3. The bright particle phases were identified as (Co, Ni)$_3$Al$_4$, an intermetallic compound combining Co and Ni with an Al. The phase formed an incoherent interface with the Al matrix [16]. The results of the XRD analysis are also shown in Fig. 4. Note that the results were different from those obtained by analyzing Al-Mg-Si alloys that have Al matrix, Mg$_2$Si particles, eutectic Si phases, and intermetallic compounds [17]. In the EDS mapping analysis (Fig. 5), Mg$_2$Si particles were usually observed in the black regions around (Co, Ni)$_3$Al$_4$ particles, and some had formed at the grain boundary or inside grains. It is noteworthy that the eutectic Si phase and Fe-based intermetallic compound were not identified in new heat-resistant aluminum alloy. DTA analysis was also conducted to investigate the thermal stability of the new heat-resistant aluminum alloy. As shown in Fig. 6, the new Al alloy maintained the initial phase without phase transformation from room temperature to 625 °C as the melting point of aluminum alloy used in this study. This suggests that the (Co,

Table 1. Tensile properties of new heat resistance Al alloy [13] and A319 [15] from R.T. to 250 °C

	Yield strength (MPa)		Tensile strength (MPa)		Elongation (%)	
	New heat resistant Al	A319	New heat resistant Al	A319	New heat resistant Al	A319
R. T.	239.4	155	255.4	210	15.7	2
130 °C	240.5	157	255.5	225	16.6	3
250 °C	225.4	150	247.0	160	17.5	2

$Ni)_3Al_4$ and Mg_2Si phases inside the alloy can maintain a stable condition even at high temperatures.

3.2. High temperature fatigue properties of the new heat-resistant Al alloy

Table 1 shows the room-temperature and high-temperature tensile properties of the new heat-resistant Al alloy and A319 alloy [15]. At 130 °C, the high cycle fatigue test condition, the yield strength was 240.5 MPa, the tensile strength was 255.5 MPa, and the elongation was 16.6%. The A319 alloy showed a yield strength of approximately 157 MPa, a tensile strength of 225 MPa, and elongation percentages of approximately 3% at 130 °C. With these results, the new heat-resistant Al alloy demonstrated superior tensile and yield strengths and higher elongation compared to the A319 alloy.

Figure 7 presents the results of the high cycle fatigue test performed at 130 °C and compared with typical Al alloys for engine piston and blocks (A319 alloy and A356 alloy [19]). The new heat-resistant Al alloy had longer fatigue life than the conventional Al alloys in all stress conditions. The fatigue limit of the A319 alloy was approximately 60 MPa, whereas that of the new heat-resistant Al alloy was two times higher (120 MPa) at 10^7 cycles; This value (120 MPa) is a fatigue limit similar to that of the A356 alloy obtained under the same experimental conditions. However, as the maximum stress increased, the fatigue life of the new heat-resistant Al alloy was relatively longer than the conventional A356 alloy. Through

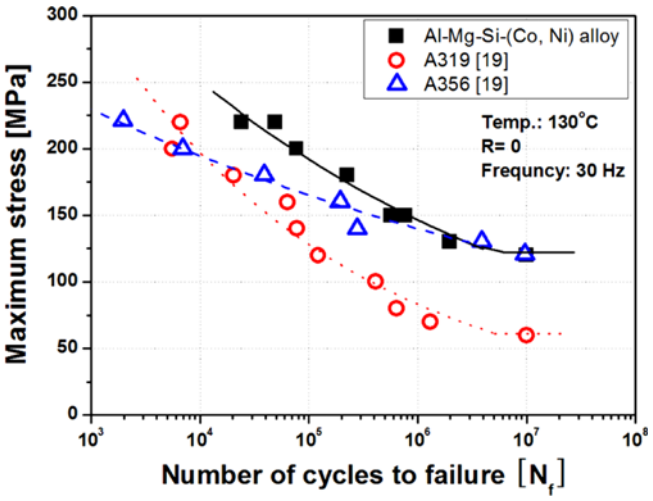

Fig. 7. High cycle fatigue results of new heat resistant Al alloy and the conventional aluminum alloys [19], tested at 130 °C.

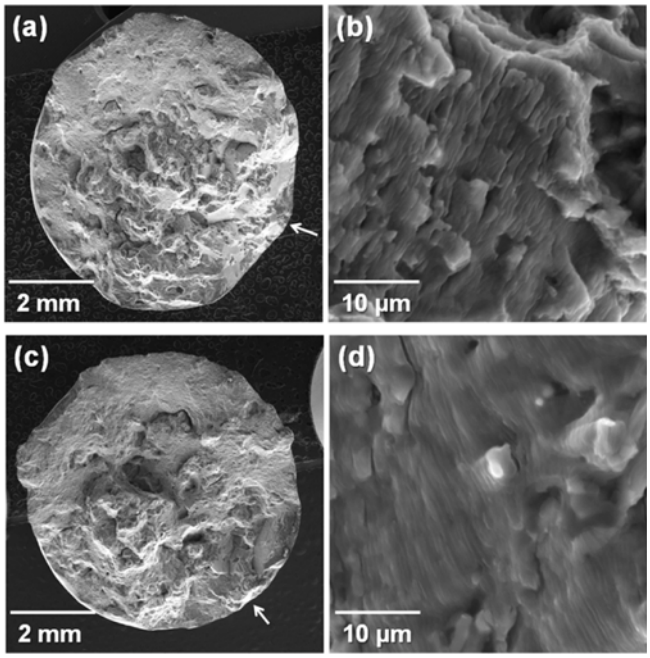

Fig. 8. Fatigue-fractured surface of Al-Mg-Si-CoNi alloy; (a-b) maximum stress at 130 MPa, and (c-d) maximum stress at 200 MPa.

these results, the high-temperature, high-cycle fatigue properties of the new heat-resistant Al alloy were confirmed to be superior to those of the conventional heat-resistant aluminum alloys. Figure 8 shows the fracture surfaces appearing under low stress and high stress conditions, respectively; fatigue crack was initiated at the points indicated by the arrows. While fatigue fracture surfaces are usually smooth and perpendicular to the stress direction, the fracture surface of the new heat-resistant Al alloy was rough, but well developed striations were found on the fatigue fracture surface (Figs. 8(b) and (d)).

Fatigue strength or fatigue life are usually determined by fatigue crack initiation and fatigue crack propagation processes, with crack initiation showing particularly significant influence on the high cycle fatigue property. It is well known that fatigue cracks can be easily initiated at the inclusion, pore, and 2nd phase near the surface [20,21]. Fatigue crack initiation sites were observed on the fatigue fracture surface, and the representative results presented in Fig. 9. The results showed that no hardening phases such as Mg_2Si and $(Co, Ni)_3Al_4$ particles or any other defects were found (Fig. 9(a)) near crack initiation sites. The cross-sections of fatigue crack

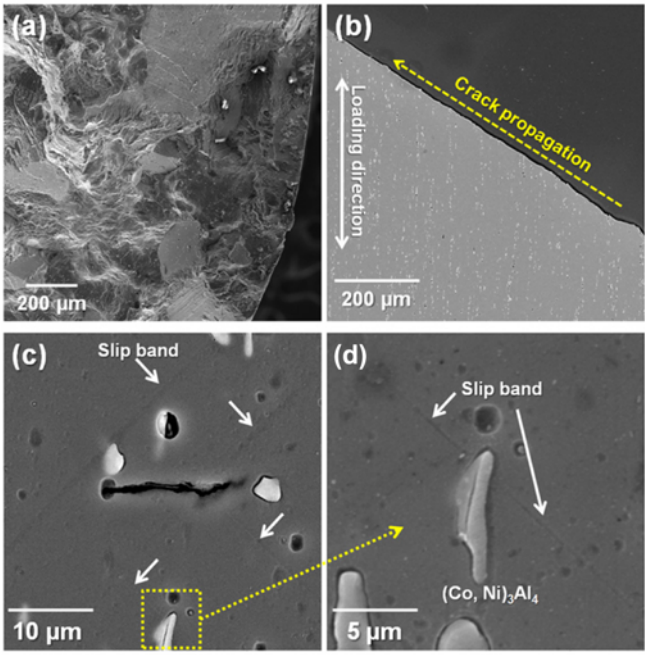

Fig. 9. Observation results of fatigue crack initiation sites; (a) crack initiation site on the fractured surface, (b) its cross sections, and (c) interactions between (Co, Ni)$_3$Al$_4$ and slip band (left) with high magnification (right).

initiation regions were examined to identify another factor that influenced fatigue crack initiation, and the results are shown in Fig. 9(b). The direction of the initiated crack caused by fatigue was approximately at a 45° angle to the applied stress. Several slip bands formed in a specific direction around the fatigue fracture surface were also noted, which was similar to the results of Henaff *et al*. [22]. Fatigue fracture of the alloy was believed to have been initiated along the persistent slip band as the typical fatigue crack initiation mechanism of the metal.

Ribes *et al.* [23] suggested that it is difficult for typical dispersion hardened particles to bond tightly with the aluminum matrix in the metal matrix composite (MMC). The discrete interface in the usual MMC can cause a significant increase of dislocation density in front of the interface and sometimes detachment between particle and matrix especially during high temperature fatigue deformation [23]. Thus, this results in a detrimental effect on the initiation and propagation of fatigue cracks [24,25]. Note, however, that the Co-Ni based reinforcing phase ((Co, Ni)$_3$Al$_4$) formed in the new alloy was created by combining Co-Ni powder and matrix aluminum; it had a highly deformation resistant interface - although incoherent [16] - unlike general-dispersed reinforcing phases. Figure 9(c) suggests that (Co, Ni)$_3$Al$_4$ particle had no detachment of interface or occurrence of shearing or cracking when the particle met slip bands during fatigue deformation. It could be assumed that the interface between (Co, Ni)$_3$Al$_4$ and Al matrix had the characteristic of precipitates, stable and effective for

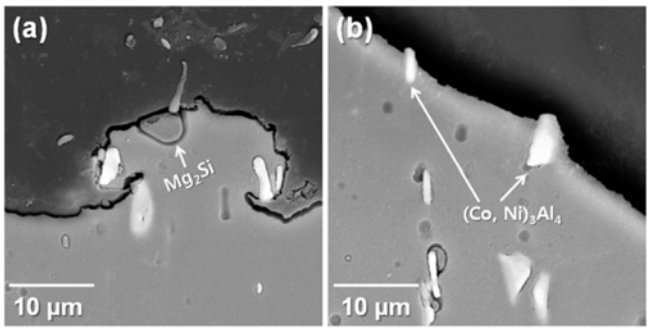

Fig. 10. SEM observation results (cross section of the fatigue-fractured surface) of the fracture of particles by fatigue crack propagation; (a) Mg_2Si phase and (b) (Co, Ni)$_3$Al$_4$ phase.

fatigue deformation, though the particle was originally designed to be a dispersion hardening one. Furthermore, the size and distribution of the (Co, Ni)$_3$Al$_4$ particles could be well controlled, since it was originated by Co-Ni powder particles. It was distributed finely and evenly in the matrix as an appropriate size of hardening particle. We believe that this new Co-Ni based particle played an effective strengthening role for improving high temperature mechanical and fatigue properties of the Al alloy.

(Co, Ni)$_3$Al$_4$ and Mg_2Si hardening phases were observed in the new heat-resistant Al alloy; the influence of these phases in fatigue crack propagation is shown in Fig. 10. Figure 10(a) illustrates the fracture of the Mg_2Si phase caused by fatigue cracks as they propagated along slip bands or grain boundaries and met the Mg_2Si phase. In this alloy, the Mg_2Si phase had a coarse appearance (above 5 μm); it was a relatively small-volume fraction compared to the (Co, Ni)$_3$Al$_4$ phase and probably has no significant influence on the enhancement of fatigue properties. The Mg_2Si phase, which was relatively smaller, likely has some reinforcing effect. Consequently, if the (Co, Ni)$_3$Al$_4$ phase encounters fatigue cracks, the cracks propagate to the interface between the reinforcing phase and the matrix as shown in Fig. 10(b), which is unlike Mg_2Si precipitates [26,27]. Since the crack direction changes as fatigue cracks propagate to the interface of the matrix and (Co, Ni)$_3$Al$_4$ phase, this is expected to reduce the crack propagation rate (improvement of high-cycle fatigue properties and reinforcement mechanism). For these reasons, the (Co, Ni)$_3$Al$_4$ phase does not have a negative influence on the fatigue crack generation but - in case of fatigue crack growth behavior - effectively changes the direction of fatigue crack propagation. Thus, we think it plays a major role in high-cycle fatigue properties.

4. CONCLUSIONS

High temperature fatigue deformation behavior of a new heat-resistant aluminum alloy was investigated in this study. The following conclusions were drawn:

(1) The new Al alloy was fabricated using powder ball milling and continuous casting processes. The alloy consisted of a primary Al matrix with an average grain size of 185 μm, a small volume fraction of Mg_2Si phases, and $(Co, Ni)_3Al_4$ particles as a reinforcing phase with a small size of 1.57 μm on average and even distribution throughout the entire alloy.

(2) The new heat-resistant Al alloy represented superior high temperature tensile properties. Comparing the high cycle fatigue properties at high temperatures of the new Al alloy to those of the A319 and A356 alloys, we found that the fatigue life was longer under all stress conditions. Furthermore, the fatigue limit (10^7 cycles) was considerably superior to the A319 alloy at 120 MPa.

(3) This alloy formed a reinforcing phase of $(Co, Ni)_3Al_4$ from the initial Co-Ni powder particles. Fine $(Co, Ni)_3Al_4$ phases distributed evenly throughout the entire alloy decreased the stress concentration and were not easily fractured by fatigue cracks. The phase likely played a role similar to that of precipitates in terms of strong bonding with the matrix, though it maintained the merits of dispersion strengthening particles (easy control of the size and distribution of strengthening particles). The $(Co, Ni)_3Al_4$ phase had effective fatigue strengthening particles on both fatigue crack initiation and crack propagation.

ACKNOWLEDGEMENT

This research was supported by a grant from the Fundamental R&D program for Core Technology of Materials funded by the Ministry of Knowledge Economy, Republic of Korea.

REFERENCE

1. W. S. Miller, L. Zhuang, J. Bottema, A. J. Wittebrood, P. De Smet, A. Haszler, and A. Vieregge, *Mater. Sci. Eng. A* **280**, 37 (2000).
2. Haizhi Ye, *J. Mater. Eng. Perform.* **12**, 288 (2003).
3. D. A. Lados and D. Apelian, *Eng. Fract. Mech.* **75**, 821 (2008).
4. R. A. Siddiqui, H. A. Abdullah, and K. R. Al-Belushi, *J. Mater. Process. Tech.* **102**, 234 (2000).
5. A. J. Moffat, S. Barnes, B. G. Mellor, and P. A. S. Reed, *Int. J. Fatigue* **27**, 1564 (2005).
6. D. Canadinc, H. J. Maier, P. Gabor, and J. May, *Mater. Sci. Eng. A* **496**, 114 (2008).
7. G. Zhang, J. Zhang, B. Li, and W. Cai, *Mater. Sci. Eng. A* **561**, 26 (2013).
8. A. M. A. Mohamed, F. H. Samuel, and S. Al kahtani, *Mater. Sci. Eng. A* **577**, 64 (2013).
9. Q. Li, T. Xia, Y. Lan, W. Zhao, L. Fan, and P. Li, *J. Alloy. Compd.* **562**, 52 (2013).
10. Y. Uematsu, K. Tokaji, and M. Kawamura, *Compos. Sci. Technol.* **68**, 2785 (2008).
11. Y. Sugimura and S. Suresh, *Metallur. Trans. A* **23**, 2231 (1992).
12. O. Hartmann, M. Kemnitzer, and H. Biermann, *Int. J. Fatigue* **24**, 215 (2002).
13. M. Papakyriacou, H. R. Mayer, S. E. Stanzl-Tschegg, and M. Groschl, *Int. J. Fatigue* **18**, 475 (1996).
14. S. B. Kim, D. A. Koss, and D. A. Gerard, *Mater. Sci. Eng. A* **277**, 123 (2000).
15. C. S. Shin and J. C. Huang, *Int. J. Fatigue* **32**, 1573 (2010).
16. S. H. Choi, S. Y. Sung, H. J. Choi, Y. H. Sohn, B. S. Han, and K. A. Lee, *Mater. Trans.* **52**, 1661 (2011).
17. S. W. Han, K. Katsumata, S. Kumai, and A. Sato, *Mater. Sci. Eng. A* **337**, 170 (2002).
18. E. Rincon, H. F. Lopez, M. M. Cisneros, H. Mancha, and M. A. Cisneros, *Mater. Sci. Eng. A* **452**, 682 (2007).
19. J. S. Park, S. Y. Sung, B. S. Han, C. Y. Jung, and K. A. Lee, *Korean J. Met. Mater.* **48**, 28 (2010).
20. R. Ammar, A. M. Samuel, and F. H. Samuel, *Mater. Sci. Eng. A* **473**, 65 (2008).
21. Q. G. Wang, D. Apelian, and D. A. Lados, *J. Light Metals* **1**, 73 (2001).
22. G. Henaff, F. Menan, and G. Odemer, *Eng. Fract. Mech.* **77**, 1975 (2010).
23. H. Ribes, M. Suery, G. L'esperance, and J. G. Legoux, *Metallur. Trans. A* **21**, 2489 (1990).
24. T. Varol and A. Canakci, *Met. Mater. Int*. **19**, 1227 (2013).
25. B.-J. Choi and Y.-J. Kim, *Met. Mater. Int*. **19**, 1301 (2013).
26. E. Rincon, H. F. Lopez, M. M. Cisneros, and H. Mancha, *Mater. Sci. Eng. A* **519**, 128 (2009).
27. P. Poza and J. Llorca, *Mater. Sci. Eng. A* **206**, 183 (1996).